

Anomalous proton-spin–lattice relaxation at high temperatures in zirconium dihydrides

J-W. Han,* D. R. Torgeson, and R. G. Barnes

Ames Laboratory, Department of Physics and Astronomy, Iowa State University, Ames, Iowa 50011

D. T. Peterson

Ames Laboratory, Department of Materials Science and Engineering, Iowa State University, Ames, Iowa 50011

(Received 16 May 1991)

Measurements of the proton-spin–lattice relaxation rate R_1 are reported for zirconium dihydrides, ZrH_x ($1.58 \leq x \leq 1.98$), with emphasis on the behavior of R_1 at high temperatures (to 1300 K). An anomalously sharp increase in R_1 is found at all hydrogen concentrations at temperatures above ~ 900 K. At the onset temperature T_c for anomalous R_1 behavior, defined as that of the intermediate R_1 minimum, the hydrogen hopping rate $\nu_c \approx 10^9$ – 10^{10} s $^{-1}$, decreasing with increasing hydrogen concentration x . The anomalous behavior depends only weakly on resonance frequency and shows no correlation with the pronounced peak in the electronic density of states at $x \approx 1.80$. No differences were found in the behavior of pure and impurity-doped (Cr, Mn, Fe) samples. The anomalous contribution to R_1 is described by $R_{1x} = A' \exp(-U/k_B T)$, with $U \approx 0.4$ – 1.0 eV/atom.

I. INTRODUCTION

The anomalous behavior of the proton (1H) spin-lattice relaxation (SLR) rate R_1 at temperatures in the range 700–1300 K has been found previously in the dihydride (MH_2) phases of Sc and Y.¹ Additional preliminary measurements showed that similar behavior occurs in the dihydrides of Ti, Zr, and La, as well.² We report here the results of a more detailed study of the proton SLR in zirconium dihydrides (ZrH_2) with emphasis on the anomalous high-temperature behavior.

The anomaly is that, in addition to the usual R_1 maximum that occurs at intermediate temperatures due to hydrogen diffusive motion, R_1 passes through a minimum and increases sharply again at higher temperatures instead of returning to the value R_{1e} determined by the conduction electron contribution to R_1 . This is clearly seen to occur in $ZrH_{1.75}$, data for which are shown in Fig. 1, and in $ZrH_{1.58}$ and $ZrH_{1.98}$, the end members of the series of samples investigated, in Fig. 2. In terms of the nuclear dipolar contribution, R_{1d} , which at high temperatures rather generally behaves as $R_{1d} \propto \tau_c$, where τ_c is the correlation time for hydrogen motion, this behavior implies that $\tau_c(T)$, and therefore the mean dwell time for the motion $\tau_d(T)$ passes through a minimum and increases again with increasing temperature. This conclusion stands in sharp contrast to that which follows from measurements of the hydrogen diffusion coefficient D at high temperatures. Measurements of D in yttrium dihydrides, using quasielastic neutron scattering (QENS),^{3,4} and in the solid solution phase of the Nb-V-H system using both QENS (Ref. 3) and NMR pulsed field gradient⁵ measurements, have found D increasing throughout the same temperature region, indicating that τ_d continues to decrease with increasing temperature normally (i.e., following Arrhenius behavior).

The anomalous high-temperature behavior of R_1 has

led to the conclusion that some, as yet unknown, SLR mechanism R_{1x} must be responsible.⁶ Various candidate mechanisms have been discussed and rejected² including (1) metal atom self-diffusion, (2) oxygen, nitrogen, etc., impurity self-diffusion, (3) paramagnetic impurities, (4) octahedral site occupancy by hydrogen, (5) chemical exchange with hydrogen in the gas phase, (6) ortho-hydrogen molecules on grain surfaces, and (7) an electronic structure transition.

The steep increase in R_1 in the anomalous region corresponds to an activation energy, $U \approx 0.4$ – 1.0 eV/atom, suggesting that the anomalous relaxation mechanism occurs in an “excited state” of some kind. Several such possibilities have been investigated: (1) a two-state model

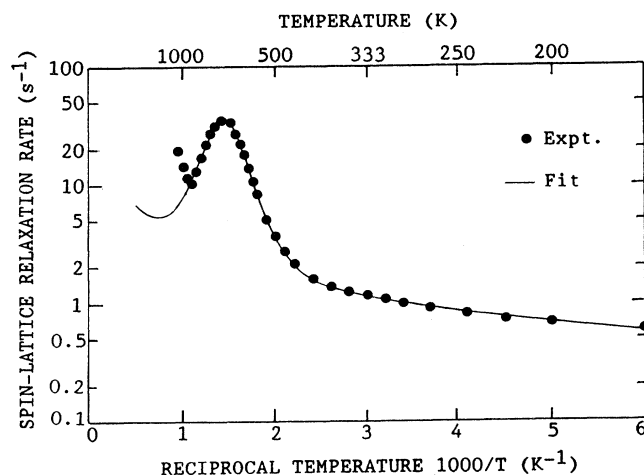


FIG. 1. A typical least-squares fit of Eq. (1) to experimental proton R_1 data in the intermediate- and high-temperature regions for $ZrH_{1.75}$ at 40 MHz, excluding the points in the region of the high-temperature anomaly.

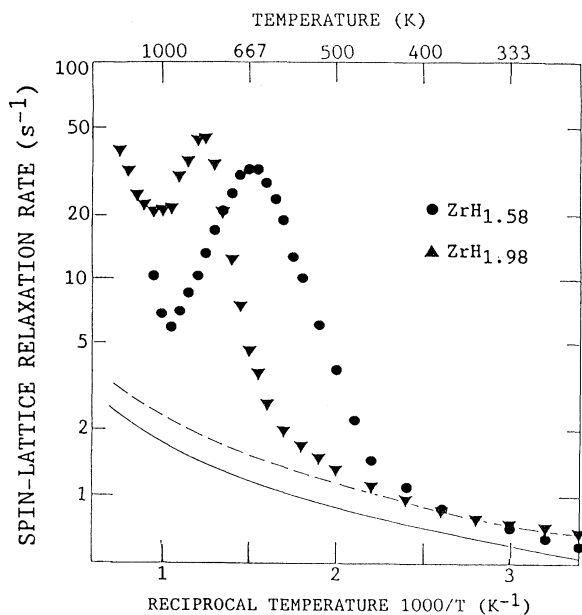


FIG. 2. Temperature dependence of the proton R_1 in ZrH_x ($x = 1.58$ and 1.98) at 40 MHz. The solid and dashed curves show the conduction electron contribution R_{1e} extended from low temperatures for $x = 1.58$ and 1.98 , respectively.

for hydrogen diffusion,⁵ (2) relaxation in deep trap states at dislocations, etc.,⁵ (3) fast relaxation in pairing states,⁶ e.g., H_2 moleculelike states, but none have proven satisfactory. Thus, the problem for experiment remains to further delineate the character of the anomalous R_1 behavior in order to provide a better focus for theoretical efforts at explanation.

Several features of ZrH_2 are significant for testing ideas relating to the anomalous proton SLR behavior. (1) The ZrH_2 phase (actually phases) exists over a substantially wider range of hydrogen concentration x than the corresponding ScH_2 and YH_2 phases. In ZrH_x , x ranges from ~ 1.4 to 2.0, whereas the lower limit in ScH_x and YH_x is ~ 1.8 . Thus, the dependence of the anomaly on x can be examined over a wider range in ZrH_x . (2) The electronic density of states (DOS) of ZrH_x varies strongly with x . The DOS at the Fermi level $N(E_F)$ passes through a sharp maximum at $x \approx 1.8$,⁷ whereas $N(E_F)$ in the Sc and Y dihydrides is essentially flat. Hence, the dependence of the anomaly on $N(E_F)$ can be examined. (3) A structural phase transition occurs from the fcc δ phase ($1.4 \leq x < 1.6$) to the fct ϵ phase ($1.6 < x \leq 2$) that is attributed to a Jahn-Teller distortion.⁷ The influence of this transition of the anomaly can also be appraised. (4) The activation energy for hydrogen diffusive motion, E_a , increases sharply as x approaches the stoichiometric limit 2, nearly doubling its value at lower x values.⁸ How this behavior of E_a influences R_1 at high temperatures can be noted. (5) In contrast to ScH_2 , in which the ^{45}Sc nuclear moment contributes strongly to the proton SLR rate,¹ the ^{91}Zr contribution to R_{1d} is negligible.⁸ If proton-proton dipolar interactions are, in fact, responsible for the anomaly, then this should be more strongly evident in ZrH_x than in ScH_x .

II. EXPERIMENT

All samples were prepared from high-purity Ames Laboratory zirconium, with purity established by spark-source mass spectroscopy. The metal was heated to 943 K for high composition samples ($1.9 < x < 2.0$) and to 1053 K for lower compositions to prepare the hydrides. The hydriding reaction was carried out by exposing the heated metal to hydrogen gas, obtained from UH_3 , in a modified Sieverts apparatus and maintaining the system at temperature for 24 h to assure equilibrium. Samples were then crushed in a mortar in a helium-filled glove box, filtered through a 200-mesh sieve, and sealed in quartz tubes under low inert-gas pressure. Compositions were initially determined from the weight gain and final hydrogen pressure, and lastly by hot vacuum extraction analysis.

Measurements of the 1H R_1 were made over the temperature range 20–1300 K at resonance frequencies in the range 12–54 MHz using a phase-coherent pulsed NMR spectrometer and associated instrumentation.⁹ Values of R_1 were obtained from fitting magnetization recovery curves resulting from measurements of the free induction decay (FID) following either a 180° inversion pulse or a saturation comb of four or five closely spaced 90° pulses. For high temperatures, a homebuilt, water-cooled furnace probe was used, and temperatures were measured with a Pt-Pt/10% Rh thermocouple.¹⁰ For low-temperature measurements a homebuilt, hydrogen-free probe¹¹ was used, with temperatures determined by a chromel-(Au+0.07 at. % Fe) thermocouple. Samples in the form of fine powder (< 200 mesh) were sealed in evacuated quartz tubes.

The temperature that can be reached in these measurements is limited either by the softening temperature of quartz or by the high hydrogen pressure developed over the metal hydride (causing the sample container to explode), or both. The transition-metal dihydrides reach high dissociation pressures well below the softening temperature of quartz, and for that reason the measurements were not pushed to the limit of sample tube explosion in every case.

III. RESULTS AND DISCUSSION

Although the anomalous SLR at high temperatures motivated this investigation, measurements were made over a wide temperature range, typically down to 20 K, in order to establish as reliably as possible the "normal" contributions to the proton SLR. These are the rates due to the conduction electron contribution R_{1e} and to the diffusion modulated dipolar interaction R_{1d} . As examples, the temperature dependence of the proton R_1 in $ZrH_{1.75}$, measured over the temperature range 170–1050 K at a resonance frequency of 40 MHz, is shown in Fig. 1, and the measured rate R_1 in $ZrH_{1.58}$ over the temperature range 45–170 K is shown in Fig. 3. The data in Fig. 1 show typical behavior in which the measured rate results from the sum of R_{1e} and R_{1d} . The dashed curve through the data points is the least-squares fit of the

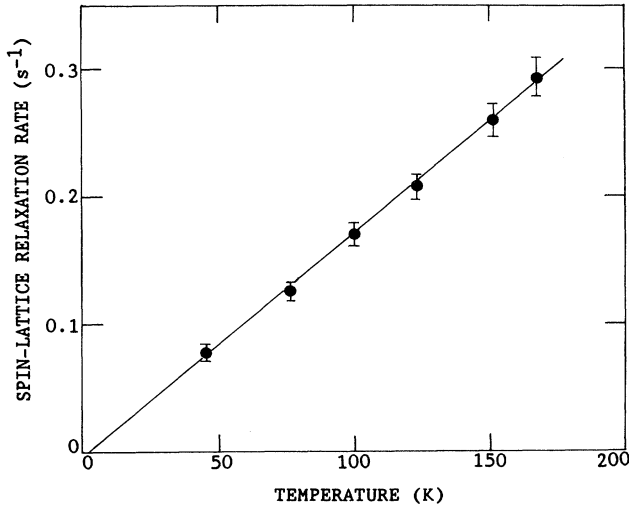


FIG. 3. Temperature dependence of the proton R_1 in $\text{ZrH}_{1.58}$ at 40 MHz (uncertainties are $\pm 5\%$).

theoretical expression for the sum of these two contributions:

$$R_1 = R_{1e} + R_{1d}, \quad (1)$$

$$R_1 = (R_{1e}/T)T + \frac{2M_2}{3\omega_0} \left[\frac{y}{1+y^2} + \frac{4y}{1+4y^2} \right].$$

In Eq. (1), M_2 is the rigid-lattice dipolar second moment at the proton site due to ^1H - ^1H interactions, ω_0 is the proton Larmor frequency, and $y = \omega_0\tau_c$, where τ_c is the correlation time. For ^1H - ^1H interactions, $\tau_c = \tau_d/2$ where τ_d is the mean dwell time of a hydrogen at an interstitial site. This formulation is based on the usual Lorentzian [so-called Bloembergen-Purcell-Pound (BPP)] spectral densities corresponding to correlation functions that decay exponentially with correlation time τ_c .¹² This procedure was used in order to permit more direct comparison with various earlier results, essentially all of which also utilized the BPP function.

The principal consequence of using the results of lattice-specific theories for the spectral densities in Eq. (1) is to change the value of $\omega_0\tau_c$ at which R_{1d} reaches its maximum value, $R_{1d,\text{max}}$. With BPP spectral densities, $\omega_0\tau_c = 0.615$ at $R_{1d,\text{max}}$, independent of hydrogen concentration x . Monte Carlo calculations, and/or the analytic representation thereof,¹³ yield x -dependent $\omega_0\tau_c$ values at $R_{1d,\text{max}}$, ranging from $\omega_0\tau_c \approx 0.4$ at $x = 1.60$ to $\omega_0\tau_c \approx 0.24$ at $x \rightarrow 2$. These changes result in somewhat smaller values of τ_c , and hence of τ_d , at $R_{1d,\text{max}}$, and lead to values of the jump attempt frequency ν_0 greater than the BPP estimate by factors of 2–2.5.

Similar fits to that in Fig. 1 were made to the data for intermediate compositions. The fitting procedure yields the Korringa parameter, R_{1e}/T ,¹⁴ and the two parameters characterizing the assumed Arrhenius behavior of the hydrogen hopping rate, i.e., the activation energy for hydrogen diffusive hopping E_a and the jump attempt fre-

quency ν_0 . In the Zr dihydrides, the quantity R_{1e}/T is related to the density of states at the Fermi level $N(E_F)$ according to

$$R_{1e}/T = (R_{1e}/T)_0 \left[1 + \frac{(\pi k_B T)^2}{3} \frac{1}{N(E)} \frac{d^2 N(E)}{dE^2} \right]_{E_F}, \quad (2)$$

where $(R_{1e}/T)_0$ is the limiting low-temperature value which, for the Zr dihydrides, can be expressed as⁷

$$(R_{1e}/T)_0 = 4\pi h \gamma k_B [H_{\text{hf}}(d)N_d(E_F)]^2 q. \quad (3)$$

In Eq. (3), $H_{\text{hf}}(d)$ is the hyperfine field at the proton resulting from core polarization of spin-paired s orbitals at energies below E_F by unpaired d electrons at E_F , $N_d(E_F)$ is the d -band DOS at the Fermi level, and q is a numerical reduction factor arising from d -band degeneracy.

At low temperatures, R_{1d} is negligible and the measured rate is expected to yield $(R_{1e}/T)_0$ directly. The straight-line fit to the data in Fig. 3 shows that this is the case. More importantly, it shows that the sample is not contaminated by paramagnetic impurities which can interfere significantly with the determinations of both R_{1e}/T and the diffusion parameters,¹⁵ and that cross relaxation to the ^{91}Zr spins is negligible.¹⁶ The latter process also interferes with the determination of R_{1e}/T . The $(R_{1e}/T)_0$, E_a , and ν_0 results are summarized in Table I.

A. Hydrogen diffusion parameters

Although several series of proton SLR measurements have been made on ZrH_x in recent years, the values of the diffusion parameters derived from these continue to differ somewhat. We compare in Fig. 4 the present and earlier results for the hydrogen concentration dependence of E_a . Our results agree well with those of Korn and Goren¹⁷ (or Pope *et al.*¹⁸) except for compositions at the stoichiometric limit. On the other hand, Bowman and Craft's values⁸ are substantially lower in comparison to the others except at the highest hydrogen concentrations. Because their results were based on $R_{1\rho}$ measurements (R_1 in the rotating frame), it was thought that R_1 and $R_{1\rho}$ may yield different E_a values, and therefore $R_{1\rho}$ was measured for the $x = 1.58$ and 1.98 samples to clarify this point. Figure 5 shows the temperature dependence of $R_{1\rho}$ (at 24 MHz) for $x = 1.98$. The results from the two methods were the same within the experimental uncertainty (see Table I).

One striking feature of the results is that E_a and ν_0 for the $x = 1.98$ sample increase dramatically compared to values for lower compositions, in fact, E_a is nearly twice as great as that for $x = 1.93$. Although the Bowman and Craft measurement for $x = 1.99$ is incomplete,⁸ their value $E_a = 1.13$ eV/atom deduced from the slope of the low-temperature side of the $R_{1\rho}$ minimum is reasonable since the R_{1e} contribution is negligible in the $R_{1\rho}$ measurement. We may infer from Fig. 4 that the rapid increase in E_a begins at $x \approx 1.93$. The value of $E_a = 0.8$ eV/atom for $x = 1.96$ given by Pope *et al.*¹⁸ supports this

TABLE I. Hydrogen hopping rate (diffusion) parameters in ZrH_x determined from R_1 and $R_{1\rho}$ measurements. Estimated uncertainties are ± 0.02 in x , ± 0.03 eV/atom in E_a , $\pm 50\%$ in ν_0 , and $\pm 3\%$ in $(R_{1e}/T)_0$.

ZrH_x x	Frequency (MHz)	E_a (eV/atom)	ν_0 (10^{12}) s^{-1}	$(R_{1e}/T)_0$ [$10^{-3}(s\ K)^{-1}$]
1.58	40.0	0.57	4.9	1.79
	12.2	0.58	5.8	
	$T_{1\rho}$	0.55	2.2	
1.75	40.0	0.56	2.2	3.45
	12.2	0.57	2.3	
1.79	40.0	0.58	2.5	4.00
	12.2	0.58	2.5	
1.86	40.0	0.60	1.8	3.45
1.91	40.0	0.63	1.9	2.70
	12.2	0.63	1.5	
1.93	40.0	0.66	2.0	2.50
	12.2	0.63	0.9	
1.98	40.0	1.06	760	2.44
	12.2	1.08	1200	
	$T_{1\rho}$	1.20	6800	

trend, whereas Korn and Goren's value¹⁷ for this composition appears too small. Bowman and Craft⁸ proposed that the rapid increase of E_a as $x \rightarrow 2$ could be attributed to an increase in vacancy formation energy.

Stalinski *et al.*¹⁹ concluded that the hopping rate is directly proportional to the vacancy concentration on the hydrogen sublattice in titanium dihydride, TiH_x , indicating that hydrogen moves via a vacancy mechanism. Korn and Goren¹⁷ extended this concept to ZrH_x and gave an explicit expression for the x dependence of their measured ν_0 values:

$$\nu_0 = [(2-x)/2](45 \pm 10) \times 10^{12} s^{-1}. \quad (4)$$

As is evident from the ν_0 values in Table I, our results do not show a steady decrease with increasing x , but are approximately constant over the ϵ -phase region except for $x = 1.98$. On the other hand, there is good order-of-

magnitude agreement between the two sets of results. In contrast, Bowman and Craft's values of ν_0 ,⁸ based on $R_{1\rho}$ measurements, are smaller by as much as 2 orders of magnitude.

In fact, the particle (i.e., hydrogen) and vacancy hopping rates, ν_p and ν_v , on the hydrogen sublattice must be related by $\nu_p = [c_v/(1-c_v)]\nu_v$, where $c_v = (2-x)/2$ is the vacancy concentration, since the flux of vacancies and particles must be the same. Thus, Eq. (4) is a first approximation to the exact result

$$\nu_p = [(2-x)/x]\nu_v. \quad (5)$$

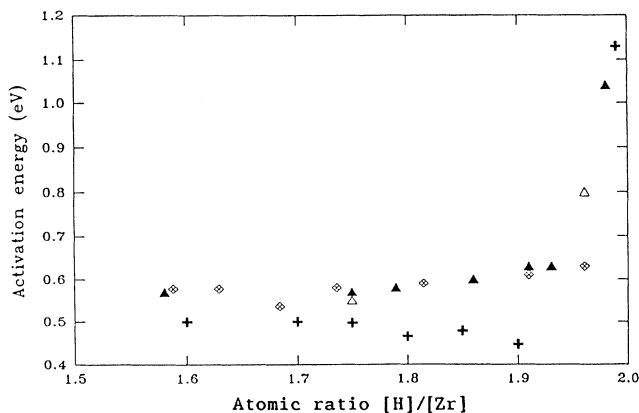


FIG. 4. Dependence of the activation energy E_a for hydrogen diffusive hopping on hydrogen concentration in ZrH_x (▲, this work; ◆, Ref. 17; +, Ref. 8; △, Ref. 18).

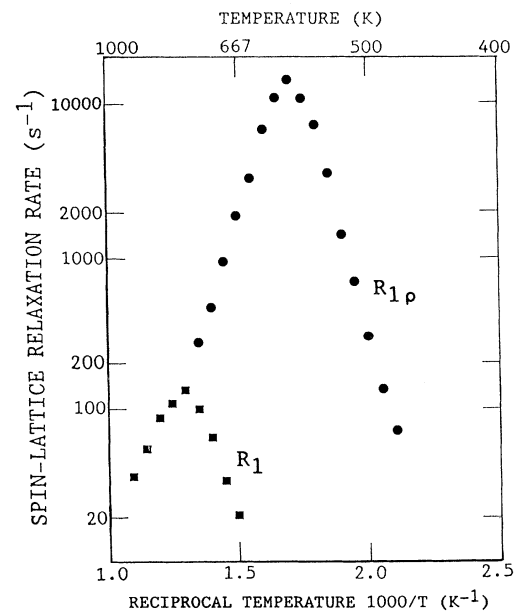


FIG. 5. Temperature dependence of the proton $R_{1\rho}$ measured at 24 MHz in $ZrH_{1.98}$. R_1 data points at 12.2 MHz are also shown.

With the exception of the results for $x = 1.98$, most of the ν_0 values are substantially less than expected on the basis of the fundamental hydrogen optical vibration energy determined by neutron-scattering measurements. Couch *et al.*²⁰ found a peak energy of 141 meV at both $x = 1.56$ and 2.00 in the dihydride phase corresponding to a frequency $\nu_0^0 = 3.4 \times 10^{13} \text{ s}^{-1}$. For a single-particle hopping on an empty lattice, the attempt frequency is given by $\nu_0 = z\nu_0^0$, where $z = 6$ is the number of neighbor sites on the simple-cubic T -site sublattice in the fcc dehydrides, so that $\nu_0 \approx 2.0 \times 10^{14} \text{ s}^{-1}$. In the present case, this would be the *vacancy* hopping rate, ν_V , as was found for Sc dihydrides²¹ on the basis of measurements of R_{1d} for the stationary ^{45}Sc nucleus which is relaxed by quadrupole interaction fluctuations due to vacancy hopping. Based on the neutron value for ν_0^0 and Eq. (5), we expect ν_0 to range from $54 \times 10^{12} \text{ s}^{-1}$ at $x = 1.58$ down to $7.2 \times 10^{12} \text{ s}^{-1}$ at $x = 1.93$ and $2.0 \times 10^{12} \text{ s}^{-1}$ at $x = 1.98$. Best agreement with the ν_0 values in Table I occurs at $x = 1.93$, and the agreement would be generally improved if lattice-specific spectral densities were used in fitting the R_{1d} data.

The simple formulation that $\nu_0 = z\nu_0^0$, elaborated above, neglects the entropy factor $\exp(S/k_B)$, where S is sum of the entropies for vacancy formation S_F and for motion S_M . The former is expected to be small when the vacancy concentration c_v is large, but may increase substantially as $x \rightarrow 2$. The ν_0 value for $x = 1.98$ is ~ 1500 times that at $x = 1.93$, and if this increase is attributed to an increased entropy factor, one obtains $S/k_B \approx 7.3$, compared to $S/k_B \approx 1.5$ at lower x values.

B. Electronic structure parameters

The temperature dependence of $(R_{1e}/T)^{1/2}$, which reflects the relative position of E_F with respect to a peak in the band structure through Eq. (2), is shown in Fig. 6. Three different situations can be summarized as follows. First, $(R_{1e}/T)^{1/2}$ values are nearly constant over the experimental temperature range for ZrH_x with $x = 1.91$, 1.93, and 1.98. This shows that $[d^2N(E)/dE^2]_{E_F}$ is negligibly small for these samples. Second, $(R_{1e}/T)^{1/2}$ values for $x = 1.75$, 1.79, and 1.86 decrease slightly with increasing temperature, indicating that the second derivatives for these samples have negative values. Finally, $(R_{1e}/T)^{1/2}$ for $x = 1.58$ decreases initially and becomes constant with decreasing temperature.

Korn²² and Bowman *et al.*^{7,23} have previously measured the proton R_{1e} and Knight shift for ZrH_x . Comparison shows that Korn's R_{1e} results are inconsistent with ours throughout the entire range of compositions, whereas those of Bowman *et al.* are generally in good agreement. For the purpose of data analysis, Eq. (2) can be written

$$R_{1e}/T = (R_{1e}/T)_0(1 + bT^2). \quad (6)$$

Values of $b \propto [d^2N(E)/dE^2]_{E_F}$ can be derived from plots of $(R_{1e}/T)T^2$ versus T in the temperature range where R_{1d} is negligible (below ~ 300 K in the Zr dihydrides).

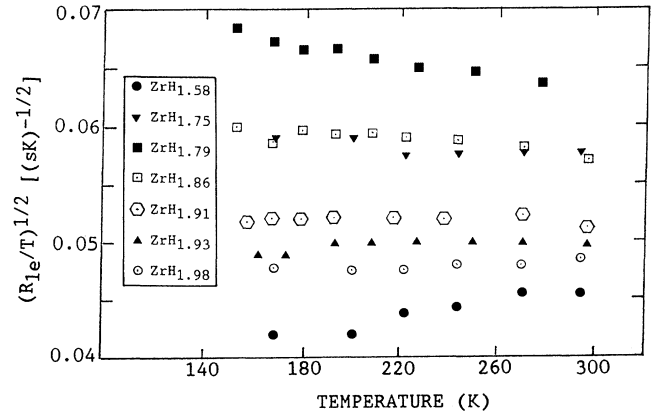


FIG. 6. Temperature dependence of $(R_{1e}/T)^{1/2}$ at various x values.

As noted by Bowman *et al.*,²³ a local maximum in $N(E_F)$ is defined by a negative second derivative, and the magnitude of this parameter directly reflects the sharpness of the peak. The values of b derived from our data are negative and agree well in magnitude with those of Ref. 18, especially in the vicinity of the peak at $x \approx 1.80$. Both aspects differ from the results of Ref. 22 where positive values of b approximately 10^3 greater in magnitude were reported. [In Ref. 22, $R_{1e}/T = (R_{1e}/T)_0 + MT^2$, so that $b = M/(R_{1e}/T)_0$.]

IV. HIGH-TEMPERATURE ANOMALY

Anomalous behavior of the proton R_1 at high temperatures was found in all Zr dihydride samples. Examples are shown in Figs. 1 and 2. The fitted curve through the $x = 1.75$ data points in Fig. 1 undershoots the measured R_1 values in the anomalous region to a significant extent, as is also the case in other systems.^{1,2,5} Similarly, the solid and dashed curves in Fig. 2 are the extensions of the Korringa rate contribution R_{1e} for $x = 1.58$ and 1.98, respectively. Modifying the conduction electron contribution to include an additional term proportional to $[d^2N(E)/dE^2]_{E_F}$, as in Eq. (5), also fails to fit the data in the anomalous region and would, in any event, necessitate an unusually strong, *positive* curvature of $N(E_F)$, rather than *negative* as determined at low temperatures. This is also the case for other systems.^{2,5}

Comparing the R_1 behavior in $\text{ZrH}_{1.98}$ (Fig. 2) with that in $\text{ZrH}_{1.58}$ (Fig. 2) and in $\text{ZrH}_{1.75}$ (Fig. 1), it is evident that the much higher value of E_a for $\text{ZrH}_{1.98}$ shifts the entire region of diffusion-dominated and anomalous behavior to higher temperatures. Thus, the R_1 maximum occurs at $T_{\text{max}} = 655$ K in $\text{ZrH}_{1.58}$ at 690 K in $\text{ZrH}_{1.75}$, and 815 K in $\text{ZrH}_{1.98}$. Likewise, the onset temperature T_c of the anomaly, defined as the temperature of the R_1 minimum before the upturn, also shifts to higher values: $T_c = 910$ K in $\text{ZrH}_{1.75}$, and in $\text{ZrH}_{1.98}$, $T_c = 1000$ K. This trend is followed throughout the entire composition range with the exception of the δ -phase sample, $x = 1.58$, for which T_c is greater than those of the $x = 1.75$ and

1.79 ϵ -phase samples. The T_{\max} and T_c values (based on the 40-MHz data) are summarized in Table II.

The temperature dependence of R_1 was also measured at high temperatures in a number of Zr dihydrides containing controlled low levels of Cr, Mn, and Fe. These had been prepared and used in a study of hydrogen anti-trapping by such dopants.²⁴ The compositions, doping levels, and frequencies at which R_1 measurements were made into the anomalous region are as follows: (1) ZrH_x : 500 ppm Mn at 12.2 MHz with $x = 1.57, 1.70, 1.97$; at 40 MHz with $x = 1.57, 1.70, 1.75, 1.85$; at 54 MHz with $x = 1.70$. (2) ZrH_x : 1000 ppm Mn at 12.2 MHz with $x = 1.85$. (3) ZrH_x : 500 ppm Cr at 12.2 MHz with $x = 1.85$; at 40 MHz with $x = 1.57, 1.85, 1.97$; at 54 MHz with $x = 1.85$. (4) ZrH_x : 500 ppm Fe at 40 MHz with $x = 1.82$. Further measurements on Fe-doped samples were not made since it had been shown²⁴ that Fe does not support a local moment in the Zr dihydrides. Anomalous behavior was observed in all cases, independent of whether or not the dopant caused anti-trapping at the specific hydrogen concentration x . Results for two Mn-doped samples are shown in Fig. 7. Anti-trapping does not occur in the low-concentration, $x = 1.57$, sample, but does in the high-concentration, $x = 1.97$, sample as evidenced by the low-temperature secondary R_1 maximum.

As noted elsewhere for other metal-hydrogen systems,² the hydrogen hopping rate $\nu_c = \tau_d^{-1} \approx 10^9 - 10^{10} \text{ s}^{-1}$ at T_c . In the present case, ν_c values range from $4.7 \times 10^9 \text{ s}^{-1}$ at $x = 1.58$ to a minimum of $0.78 \times 10^9 \text{ s}^{-1}$ at $x = 1.93$. The ν_c values for the pure samples are included in Table II. They would be increased by factors in the range 2–2.5 if lattice-specific spectral densities¹³ were used in fitting R_{1d} data, thereby resulting in correspondingly greater values of the attempt frequency ν_0 . The ν_c values decrease gradually with increasing hydrogen concentration x (except for $x = 1.98$). Such behavior might be expected if the mechanism responsible for R_{1x} depends on the proton-proton dipolar interaction in an "excited state," in which close pairs are briefly formed.⁶ However, based on the present data, it does not appear possible to determine where such pairs may be located, i.e., in T -site vacancies or in larger spaces, e.g., metal-atom vacancies.²⁵ The fact that ν_c for the fcc δ -phase sample ($x = 1.58$) is not in line with the fct ϵ -phase values may indicate that the structural difference exerts a small influence on the anomalous behavior.

alous behavior.

R_1 measurements were made at 12.2 and 40 MHz and, in several cases, at 54 MHz as well. In all cases, a weak frequency dependence of R_1 was observed in the anomalous region. This behavior is seen in Fig. 8 which shows the temperature dependence of R_1 in $ZrH_{1.75}$ at the three frequencies. At 1000 K, the rate $R_{1x} \propto \omega^{-0.35}$, approximately. This is nearly frequency independent, as would be expected in the short-correlation-time regime, and certainly much weaker than the ω^{-2} dependence expected in the long-correlation-time regime for BPP spectral densities.

It was previously shown for the proton R_1 in the solid solution phases of the group-V metal-hydrogen systems⁵ that the anomalous high-temperature behavior can be fit phenomenologically by adding a term of the form $R_{1x} = A' \exp(-U/k_B T)$ to Eq. (1). Such a term suggests that the anomalous relaxation occurs in an excited state of some kind, as yet undetermined, as described briefly in the Introduction. Entirely similar behavior is seen in the present results for the Zr dihydrides. Shown in Fig. 9 are the high-temperature R_1 data for $x = 1.98$ at 40 MHz after subtracting the Korringa rate $R_{1e} = T/410 \text{ s}^{-1}$ from the measured values. Measurements on this sample were made to a higher temperature, 1333 K, than on most other samples. (Unfortunately, the quartz sample tube exploded.) The entire range of high-temperature behavior, including the normal R_1 minimum, is described by

$$R_1 - R_{1e} = R_{1d} + A' \exp(-U/k_B T), \quad (7)$$

where R_{1d} is given in Eq. (1). The solid curve through the data points is the least-squares fit of Eq. (7) with $U = 0.41 \text{ eV/atom}$ and $A' = 1.39 \times 10^3 \text{ s}^{-1}$, and with $E_a = 1.06 \text{ eV/atom}$ and $\nu_0 = 7.6 \times 10^{14} \text{ s}^{-1}$ from Table I. The dashed lines in Fig. 9 show the continuation of R_{1d} to temperatures above the normal R_{1d} maximum and of R_{1x} to temperatures below the onset temperature T_c . For this composition ($x = 1.98$) and resonance frequency (40 MHz), the anomalous rate affects the total R_1 on the high-temperature side of the normal maximum, so that the high-temperature side slope is clearly weaker than the low-temperature side slope. This is already evident in Fig. 2. This effect is not so noticeable in the measurements at the lower resonance frequency of 12.2 MHz

TABLE II. Onset temperatures T_c of the anomaly, hydrogen hopping rates ν_c , and relaxation rates R_{1x} at T_c , and R_{1x} at 1000 K in ZrH_x , based on measurements at 40 MHz. Values of the temperature T_{\max} , of the (normal) dipolar R_1 maximum are also included. The estimated uncertainties are ± 0.02 in x , $\pm 15 \text{ K}$ in T_c and T_{\max} , $\pm 50\%$ in ν_c , and $\pm 8\%$ in R_{1x} .

ZrH_x x	T_{\max} (K)	T_c (K)	ν_c (10^9 s^{-1})	$R_{1x}(T_c)$ (s^{-1})	R_{1x} (10^3 K) (s^{-1})
1.58	655	950	4.7	2.6	3.9
1.75	700	910	1.8	3.1	7.4
1.79	715	910	1.5	4.5	6.5
1.86	770	950	1.2	9.3	7.0
1.91	800	950	0.87	8.5	6.9
1.93	835	975	0.78	9.7	11.3
1.98	815	1000	3.5	14.3	14.3

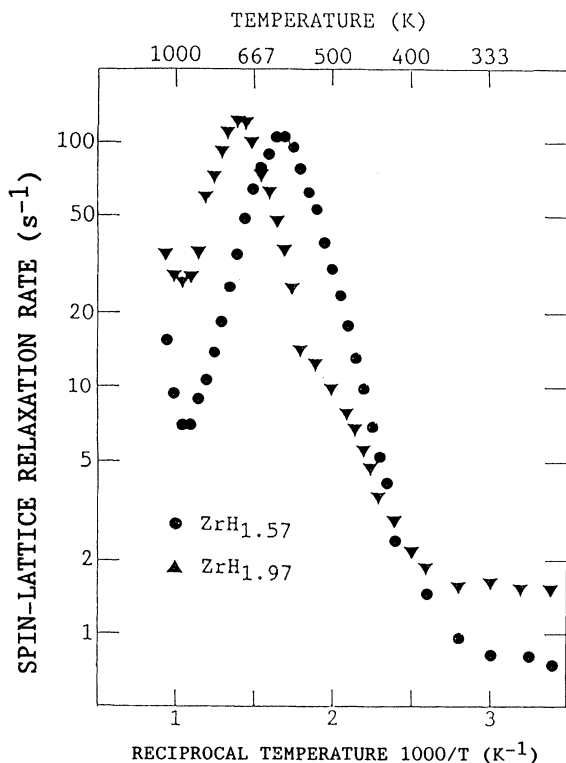


FIG. 7. Temperature dependence of proton R_1 measured at 12.2 MHz in ZrH_x ($x=1.57$ and 1.97) containing 500 ppm Mn impurity.

where the normal R_1 maximum is substantially deeper [see Fig. 7, for example].

It is also evident from Figs. 2 and 7 that the activation energy U of the anomalous rate is much weaker at $x=1.98$ than at $x=1.58$. For $x=1.58$, $U \approx 1.0$

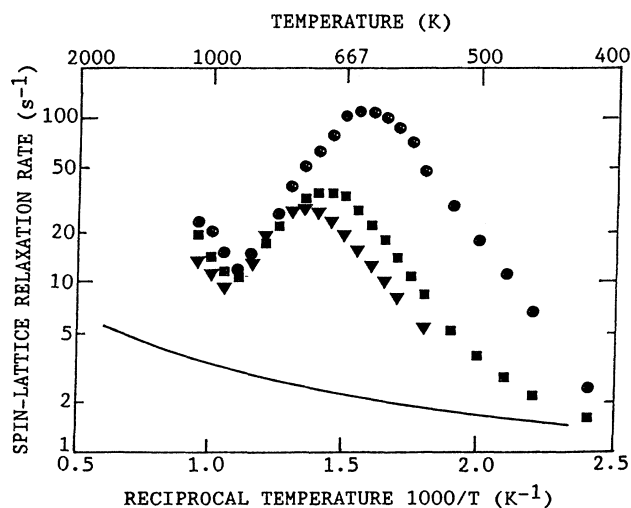


FIG. 8. Temperature dependence of the proton R_1 for $ZrH_{1.75}$ at three resonance frequencies; \bullet at 12.2 MHz, \blacksquare at 40 MHz, \blacktriangledown at 54 MHz. The solid curve is the conduction electron contribution to R_1 based on $T/R_{1e} = 290$ s K (Table I).

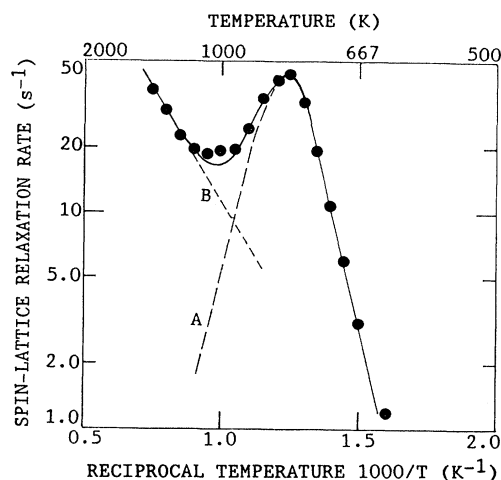


FIG. 9. Temperature dependence of the spin-lattice relaxation rate, for $x=1.98$ at 40 MHz, after subtracting the electronic contribution R_{1e} . The solid curve is the fit of the sum of the dipolar and anomalous contributions to the data points, i.e., $R_{1d} + R_{1x}$, using the parameter values given in the text. The dashed lines A and B show the extended behavior of R_{1d} and R_{1x} , respectively.

eV/atom, whereas $U \approx 0.4$ eV/atom already at $x=1.79$ and remains at approximately that value at higher compositions. The prefactor A' at $x=1.58$ also differs substantially from that at the higher compositions. At $x=1.58$, $A' \approx (2 \pm 1) \times 10^6$ s $^{-1}$, whereas at all higher compositions, $A' \approx (2.2 \pm 0.8) \times 10^3$ s $^{-1}$. These differences suggest that structure plays a role in determining the anomalous rate in this system, since the low- x compositions are in the cubic phase region while the higher compositions are all tetragonal.

The anomalous rate does not depend strongly on hydrogen concentration until $x \approx 1.93$, when the activation energy E_a for hopping starts to increase. Included in Table II are values of R_{1x} , calculated by subtracting the rates R_{1e} and R_{1d} from the measured rate R_1 . Two sets of such R_{1x} values are listed: the first set is for $T=T_c$, and the second is for $T=1000$ K. Although the values at T_c increase steadily with increasing x , this must be regarded as a consequence of the fact that T_c is itself steadily increasing, causing R_{1d} to decrease. On the other hand, when R_{1x} is calculated at a fixed temperature (1000 K) in the anomalous region, the values remain essentially constant over most of the tetragonal phase region. An increase occurs between the cubic phase ($x=1.58$) value and that at $x=1.75$, suggesting again that the structural change may influence the anomalous rate. And as remarked above, another substantial increase occurs at $x=1.93$ when the increase in E_a first becomes apparent. Both the decreasing trend of the ν_c values and the generally increasing trend of the R_{1x} values are independent of the marked change that occurs in the Korringa parameter R_{1e}/T which ranges from 1.79×10^{-3} (s K) $^{-1}$ at $x=1.58$ to a maximum of 4.00×10^{-3} (s K) $^{-1}$ at $x=1.79$ and back to 2.44×10^{-3}

(s K)⁻³ at $x = 1.98$, as the peak in $N(E_F)$ is traversed. Thus, there appears to be no evident relation between the anomalous R_1 behavior and the electronic density of states, $N(E_F)$.

V. SUMMARY AND CONCLUSIONS

Measurements of the proton R_1 in ZrH_x ($1.58 \leq x \leq 1.98$) have been made at resonance frequencies of 12.2 and 40 MHz over the temperature range 20–1100 K, and, in some cases, to 1330 K. This wide temperature range ensures that reliable values of the electronic and diffusion-modulated dipolar contributions to the relaxation rate are obtained, and that the high quality of the samples studied is confirmed. The parameters obtained in this work agree well with those obtained previously by Korn and Goren,¹⁷ by Bowman *et al.*,^{7,23} and by Bowman and Craft.⁸ In particular, the previously reported⁸ sharp increase in activation energy E_a for hydrogen diffusive hopping as $x \rightarrow 2$ is confirmed by both R_1 and $R_{1\rho}$ measurements at $x = 1.98$.

Anomalous behavior of R_1 was found to occur at all compositions at temperatures above ~ 900 K. No differences were found in the behavior of pure and

paramagnetic impurity (Cr, Mn, Fe) doped samples. The onset temperature, T_c , for anomalous behavior increases from 910 to 1000 K as x increases from 1.75 to 1.98 within the ϵ -phase region, whereas the hopping rate ν_c at T_c decreases from $\sim 1.8 \times 10^9$ s⁻¹ at $x = 1.75$ to $\sim 0.8 \times 10^9$ s⁻¹ at $x = 1.93$. Anomalous behavior depends only weakly on resonance frequency and shows no correlation with the pronounced peak in the electronic density of states at $x \simeq 1.80$. The anomalous contribution to the measured rate can be fit phenomenologically by adding a term $R_{1x} = A' \exp(-U/k_B T)$ to the usual sum of electronic and diffusion-modulated dipolar rate contributions. Values of U range from ~ 1.0 eV/atom at $x = 1.58$ down to ~ 0.4 eV/atom at $x = 1.98$.

ACKNOWLEDGMENTS

The authors are indebted to Ardis Johnson for his careful preparation and analysis of the samples. Ames Laboratory is operated for the U.S. Department of Energy by Iowa State University under Contract No. W-7405-Eng-82. This work was supported by the Director for Energy Research, Office of Basic Energy Sciences.

*Present address: Time Laboratory, Korean Standards Research Institute, Taejon, Republic of Korea.

¹R. G. Barnes, F. Borsa, M. Jerosch-Herold, J-W. Han, M. Belhoul, J. Shinar, D. R. Torgeson, D. T. Peterson, G. A. Styles, and E. F. W. Seymour, *J. Less-Common Met.* **129**, 279 (1987).

²R. G. Barnes, *Z. Phys. Chem. NF* **164**, 841 (1989).

³K. J. Barnfather, G. A. Styles, E. F. W. Seymour, A. J. Dianoux, D. R. Torgeson, and R. G. Barnes, *Z. Phys. Chem. NF* **164**, 935 (1989).

⁴U. Stuhr, M. Schlereth, D. Steinbinder, and H. Wipf, *Z. Phys. Chem.* **164**, 929 (1989).

⁵J-W. Han, L. R. Lichty, D. R. Torgeson, E. F. W. Seymour, R. G. Barnes, J. L. Billeter, and R. M. Cotts, *Phys. Rev. B* **40**, 9025 (1989).

⁶R. M. Cotts, *J. Less-Common Met.* **172**, 467 (1991).

⁷R. C. Bowman, Jr., E. L. Venturini, B. D. Craft, A. Attala, and D. B. Sullenger, *Phys. Rev. B* **27**, 1474 (1983).

⁸R. C. Bowman, Jr. and B. D. Craft, *J. Phys. C* **17**, L477 (1984).

⁹The NMR spectrometer employed a programmable pulse sequencer: D. J. Adduci and B. C. Gerstein, *Rev. Sci. Instrum.* **50**, 1403 (1979); a double sideband rf switch; D. R. Torgeson and D. J. Adduci (unpublished); and NMR receiver following the design of D. J. Adduci, P. A. Hornung, and D. R. Torgeson, *Rev. Sci. Instrum.* **47**, 1503 (1976); a variable temperature chamber with a vacuum-jacketed counterflow heat-exchanger design for $100 < T < 800$ K; D. R. Torgeson (unpublished); and a three-term programmable temperature control; D. R. Torgeson (unpublished).

¹⁰M. Jerosch-Herold, Ph.D. dissertation, Iowa State University,

1986.

¹¹L. R. Lichty, Ph.D. Dissertation, Iowa State University, 1988.

¹²N. Bloembergen, E. M. Purcell, and R. V. Pound, *Phys. Rev.* **73**, 679 (1948).

¹³C. A. Sholl, *J. Phys. C* **21**, 319 (1988).

¹⁴J. Korringa, *Physica* **16**, 601 (1950).

¹⁵T-T. Phua, B. J. Beaudry, D. T. Peterson, D. R. Torgeson, R. G. Barnes, M. Belhoul, G. A. Styles, and E. F. W. Seymour, *Phys. Rev. B* **28**, 6227 (1983).

¹⁶L. R. Lichty, J-W. Han, D. R. Torgeson, R. G. Barnes, and E. F. W. Seymour, *Phys. Rev. B* **42**, 7734 (1990).

¹⁷C. Korn and S. D. Goren, *Phys. Rev. B* **33**, 68 (1986).

¹⁸J. M. Pope, P. P. Narang, and K. R. Doolan, *J. Phys. Chem. Solids* **42**, 519 (1981); K. R. Doolan, P. P. Narang, and J. M. Pope, *J. Phys. F* **10**, 2073 (1980).

¹⁹B. Stalinski, C. K. Coogan, and H. S. Gutowsky, *J. Chem. Phys.* **34**, 1191 (1961).

²⁰J. G. Couch, O. K. Harling, and L. C. Clune, *Phys. Rev. B* **4**, 2675 (1971).

²¹M. Jerosch-Herold, L-T. Lu, D. R. Torgeson, D. T. Peterson, R. G. Barnes, and P. M. Richards, *Z. Naturforsch. Teil A* **40**, 222 (1985).

²²C. Korn, *Phys. Rev. B* **28**, 95 (1983).

²³R. C. Bowman, Jr., B. D. Craft, J. S. Cantrell, and E. L. Venturini, *Phys. Rev. B* **31**, 5604 (1985).

²⁴J-W. Han, D. R. Torgeson, and R. G. Barnes, *Phys. Rev. B* **42**, 7710 (1990).

²⁵P. Nordlander, J. K. Norskov, F. Besenbacher, and S. M. Myers, *Phys. Rev. B* **40**, 1990 (1989).